*Acknowledgment:* The authors would like to thank A. Okamoto for preparation of the MBE wafers, and T. Ozawa and K. One for implementation of the ion implantation. The authors would also like to thank H. Sakuma and Y. Takayama for their invaluable support in this work.

S. TANAKA
M. MADIHIAN
H. TOYOSHIMA
N. HAYAMA
K. HONJO

*NEC Corporation*
*4-1-1 Miyazaki*
*Miyamae-ku, Kawasaki 213, Japan*

*30th March 1987*

## References

1 NAGATA, K., NAKAJIMA, O., NITTONO, T., ITO, H., and ISHIBASHI, T.: 'Self-aligned AlGaAs/GaAs HBT with InGaAs emitter cap layer', *Electron. Lett.*, 1987, **23**, pp. 64–65

2 OSHIMA, T., ISHII, K., YOKOYAMA, N., FUTATSUGI, T., FUJII, T., and NISHI, H.: 'A self-aligned GaAs/AlGaAs heterojunction bipolar transistor with V-groove isolated planar structure'. Tech. dig. of 1985 IEEE GaAs IC symp., 1985, pp. 53–56

3 CHANG, M. F., ASBECK, P. M., MILLER, D. L., and WANG, K. C.: 'GaAs/(GaAl)As heterojunction bipolar transistors using a self-aligned substitutional emitter process', *IEEE Electron Device Lett.*, 1986, **EDL-7**, pp. 8–10

4 EDA, K., INADA, M., OTA, Y., NAKAGAWA, A., HIROSE, T., and YANAGIHARA, M.: 'Emitter-base-collector self-aligned heterojunction bipolar transistors using wet etching process', *ibid.*, 1986, **EDL-7**, pp. 694–696

# MICROWAVE TOMOGRAPHY: AN ALGORITHM FOR CYLINDRICAL GEOMETRIES

*Indexing terms: Biomedical electronics, Tomography*

The letter presents an efficient algorithm in cylindrical co-ordinates for microwave diffraction tomography. In comparison with algorithms in cartesian co-ordinates, the mechanical rotation of the object is avoided and higher-quality images are obtained with similar processing time.

*Introduction:* The goal of diffraction tomography is to reconstruct the properties of a slice of an object from scattered field measurements. Reconstruction algorithms have been usually developed for planar geometry, where a plane wave impinges on an object and the scattered fields are measured over a straight line parallel to the incident wavefront. This classical tomographic geometry requires a mechanical rotation of the object to obtain data for different directions of illumination.

However, cylindrical imaging systems have the advantage over planar ones that the encircling characteristic of the antenna is more adapted to the diffraction process in lossy objects, such as the human body. Moreover, using a synthetic aperture approach, the mechanical rotation of the object can be avoided.

At present, we are developing a cylindrical system for microwave tomography.[1] This letter presents the reconstruction algorithm and a computer simulation.

*Electromagnetic analysis:* We shall restrict our attention here to bidimensional problems, that is objects and electromagnetic fields with properties varying only over the $x$-$y$ plane. If vertically polarised antennas in the $z$-axis direction are used, all electric field and current vectors are $z$-directed, and accordingly we can use scalar field equations.

The object profile $o(\bar{r})$ is the quantity to be determined in diffraction tomography, and is related to the complex permittivity of the object $\varepsilon(\bar{r})$ through the equation

$$o(\bar{r}) = 1 - \frac{\varepsilon(\bar{r})}{\varepsilon_0} \tag{1}$$

where $\varepsilon_0$ is the complex permittivity of the medium surrounding the object.

To obtain the relationship between the scattered field and the scattering object, one must solve the inhomogeneous Helmholtz equation

$$(\nabla^2 + K_0)\psi(\bar{r}) = K_0^2\, o(\bar{r})\psi(\bar{r}) \tag{2}$$

where $K_0$ is the wavenumber of the field in the medium surrounding the object and $\psi(\bar{r})$ is the total field—incident and scattered.

When the object is illuminated by an incident plane wave propagating in direction $\hat{s}_0$, the plane wave scattering amplitude of the object is defined via eqn. 2:

$$f(\hat{s}; \hat{s}_0) = K_0^2 \iint o(\bar{r})\psi(\bar{r}; \hat{s}_0) \exp\,[-jK_0\,\hat{s}\,.\,\bar{r}]\; d^2r \tag{3}$$

where $\psi(\bar{r}; \hat{s}_0)$ is the total field, and $\hat{s}$ and $\hat{s}_0$ are the two-dimensional unit vectors defined by the angles $\chi$ and $\chi_0$, shown in Fig. 1.

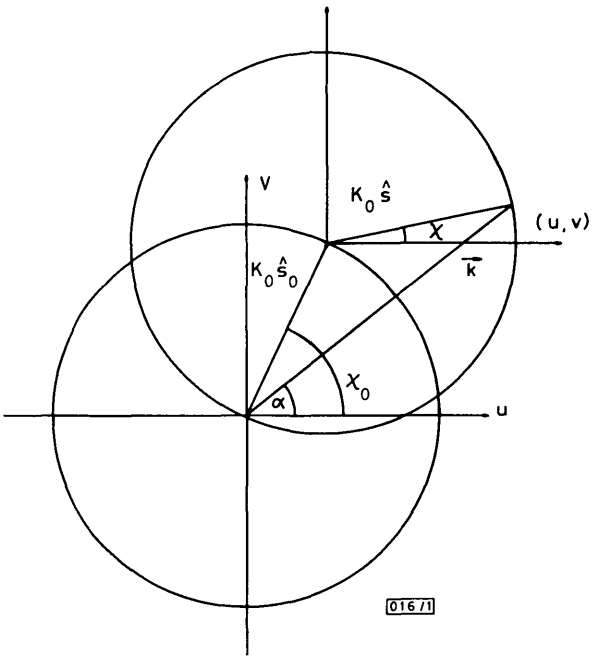


**Fig. 1** *Spectral domain of object within Born approximation*

It is difficult to solve eqn. 2 exactly. However, under the assumption of weak scattering one may use the well known Born approximation, replacing in the right-hand sides of eqns. 2 and 3 the total field by the incident one.

Then, $f(\hat{s}; \hat{s}_0)$ reduces to the bidimensional spatial Fourier transform $O(\bar{r})$ of the object evaluated over circles of radius $K_0$ in the Fourier space as shown in Fig. 1:

$$f(\hat{s}; \hat{s}_0) \sim K_0^2 \iint o(\bar{r}) \exp\,[-jK_0(\hat{s} + \hat{s}_0)\,.\,\bar{r}]\; d^2r$$

$$= K_0^2\, O(K_0(\hat{s} + \hat{s}_0)) \tag{4}$$

Using the reciprocity theorem, the plane wave scattering amplitude can be obtained from the scattered field measured along an arbitrarily shaped cylindrical antenna, that in this work will be taken as circular. Accordingly

$$\iint \frac{1}{jw\mu_0} K_0^2\, O(\bar{r})\psi(\bar{r}; \hat{s}_0) \exp\,[-jK_0\,\hat{s}\,.\,\bar{r}]\; d^2\bar{r}$$

$$= \int_0^{2\pi} I(\chi - \sigma)\psi^s(\sigma; \hat{s}_0) R\; d\sigma \tag{5}$$

where $I(\chi - \sigma)$ is the amplitude of the current distribution at an angular position $\sigma$ along the circular antenna, that, when acting as transmitter, produces a plane wave that propagates in the direction $\hat{s}$; and $K_0^2\, o(\bar{r})\psi(\bar{r}; \hat{s}_0)/jw\mu_0$ are the electric equivalent currents in the object, that produce the scattered field $\psi^s$.

When the incident field is a cylindrical wave, we can synthesise the incident plane wave as a superposition of cylindrical waves generated by line sources $I(\chi_0 - \sigma_0)$, located at positions $\sigma_0$ on the circular antenna.

Therefore, the scattered field produced by an incident plane wave, measured along the antenna, can be expressed as

$$\psi^s(\bar{r}; \hat{s}_0) = \int_0^{2\pi} I(\chi_0 - \sigma_0)\psi^s(\sigma; \sigma_0)R \, d\sigma_0 \tag{6}$$

where $\psi^s(\sigma; \sigma_0)$ is the scattered field measured at angular position $\sigma$, generated by an incident cylindrical wave produced by a unit source located at angular position $\sigma_0$.

From eqns. 3, 5 and 6 we finally obtain

$$f(\hat{s}; \hat{s}_0) = jw\mu_0 R^2 \int_0^{2\pi}\int_0^{2\pi} \psi^s(\sigma; \sigma_0) \times I(\chi - \sigma)I(\chi_0 - \sigma_0) \, d\sigma \, d\sigma_0 \tag{7}$$

*Discrete algorithm:* Instead of a circular antenna we have a circular array of $N$ omnidirectional antennas in the $x$-$y$ plane. A sampling of $\psi^s(\sigma; \sigma_0)$, $\psi^s(n; n_0)$ can be obtained, transmitting alternatively with each antenna and receiving each time with the other $N - 1$ antennas.

The discrete version of eqn. 7,

$$f(m; m_0) = jw\mu_0 R^2\left(\frac{2\pi}{N}\right) \times \sum_{n=0}^{2\pi}\sum_{n_0=0}^{2\pi} \psi^s(n; n_0)I(m - n)I(m_0 - n_0) \tag{8}$$

gives samples of $f(s; s_0)$ equispaced along complete circles.

This feature makes the difference between cylindrical and planar geometry algorithms. In the latter, samples of $f(\hat{s}; \hat{s}_0)$ are not equispaced, and cover only semicircles instead of circles.[2] Accordingly, the reconstructed object is a lowpass-filtered version of the original, being determined up to a maximum spatial frequency of $\sqrt{(2)}K_0$ with conventional planar geometry algorithms and up to $2K_0$ with cylindrical geometry ones, providing a better image resolution.

Eqn. 8 can be efficiently implemented with an FFT algorithm. Since the bidimensional discrete Fourier series of $I(\gamma)I(\gamma_0)$ is

$$\left(\frac{2}{\pi w\mu_0 R}\right)^2 \frac{j^{-(n+n_0)}}{H_n^2(K_0 R)H_{n_0}^2(K_0 R)} \tag{9}$$

$f(m; m_0)$ can be obtained with only two $N \times N$ bidimensional FFTs.

*Results:* Simulation results have been obtained with a Hewlett-Packard 9000 series 500 computer for a circular array of $N = 64$ antennas and a radius nine wavelengths long, requiring a CPU time of about 20 s.

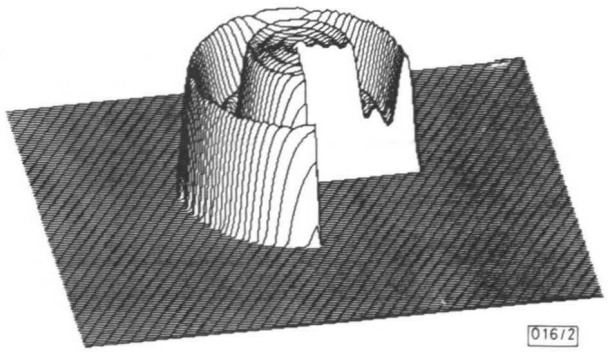


**Fig. 2** *Reconstruction of three concentric cylinders*
$r < 1{\cdot}76$, $\sigma(r) = 0{\cdot}92$
$1{\cdot}76 < r < 2{\cdot}96$, $\sigma(r) = 0{\cdot}27$
$2{\cdot}96 < r < 3{\cdot}53$, $\sigma(r) = 0{\cdot}93$

Fig. 2 shows a 128 × 128 reconstruction of a simulated test object using the Born approximation to obtain the scattered fields.

J. M. RIUS
M. FERRANDO
L. JOFRE
E. DE LOS REYES
A. ELIAS
A. BROQUETAS

*Dept. Electrofisica*
*ETSI Telecomunicacion*
*08080 Barcelona, Spain*

*2nd March 1987*

### References

1 JOFRE, L., DE LOS REYES, E., FERRANDO, M., ELIAS, A., ROMEU, J., BAQUERO, M., and RIUS, J. M.: 'A cylindrical system for quasi-real time microwave tomography'. 16th European microwave conference, Dublin, Ireland, 8–12 Sep. 1986, pp. 599–604

2 DEVANEY, A. J., and BEYLKIN, G.: 'Diffraction tomography using arbitrary transmitter and receiver surfaces', *Ultrason. Imaging*, 1984, **6**, pp. 181–193

## EFFICIENT CALCULATION OF PARTIAL DERIVATIVES IN NONLINEAR CONDUCTANCES DRIVEN BY PERIODIC INPUT SIGNALS

*Indexing terms: Microwave circuits and systems, Nonlinear systems*

Expressions for calculating current derivatives efficiently with respect to voltage in nonlinear conductances under periodic excitation are derived. The validity of Egami's approach for computing these derivatives is discussed.

Frequency-domain analysis of nonlinear circuits driven by periodic input signals reduces to the solution of a nonlinear algebraic equation system.[1] Although alternative iteration procedures[2–6] have been proposed for solving this nonlinear system, the Newton–Raphson method and minimisation techniques provide the most efficient algorithms. However, these two techniques require partial derivatives of current (voltage) phasors with respect to real and imaginary parts of voltage (current) phasors for all the nonlinear elements, this being the major drawback of these two methods because of the high computational cost of the associated calculations.

An interesting approach[7] simplifies significantly the calculation of these derivatives in the case of voltage-controlled nonlinear conductances by reducing it to the determination of the Fourier coefficients of the incremental conductance. However, it was not realised[7] that this procedure for computing the partial derivatives requires current phasors to be analytic functions of voltage phasors. In this letter correct expressions for calculating the partial derivatives associated with a voltage-controlled nonlinear conductance are obtained and discussed.

Let $i(v)$ be the nonlinear characteristic of a voltage-controlled nonlinear conductance. Under periodic excitation, current and voltage can be expressed as

$$\left.\begin{aligned} i(t) &= \sum_{k=-\infty}^{\infty} I_k \exp(jk\omega_0 t) \\ &= \sum_{k=-\infty}^{\infty} (I_k^r + jI_k^i) \exp(jk\omega_0 t) \\ v(t) &= \sum_{k=-\infty}^{\infty} V_k \exp(jk\omega_0 t) \\ &= \sum_{k=-\infty}^{\infty} (V_k^r + jV_k^i) \exp(jk\omega_0 t) \end{aligned}\right\} \tag{1}$$

(If $i(t)$ and $v(t)$ are real, as is the case of signals in nonlinear circuits, then $V_{-k} = V_k^*$ and $I_{-k} = I_k^*$.) The required partial